

Fig. 2 Proposed fully-differential SI circuit.

$$= (\alpha_1 - \alpha_2) i_{in} + \left(\frac{1}{\alpha_1} - \frac{1}{\alpha_2} \right) \frac{\beta_1}{2} V_c^2. \quad (6)$$

It should be mentioned that while the memory cell cancels the signal-dependent CFT component, the constant CFT component is left uncanceled.

Figure 2 shows the proposed fully-differential SI circuit. It consists of the two SI memory cells described above and current summing circuits which take the difference between i_1 and i_2 . Assuming matched memory cells and matched summing circuits, the output currents are given by

$$i_{out}^+ = i_1 - i_2 = (\alpha_1 - \alpha_2) (i_{in}^+ - i_{in}^-), \quad (7)$$

$$i_{out}^- = i_2 - i_1 = -(\alpha_1 - \alpha_2) (i_{in}^+ - i_{in}^-), \quad (8)$$

where i_{in}^+ and i_{in}^- are the differential input signals including the common-mode (CM) component. The current summing circuits thus cancel the constant CFT component and CM signal. The signal-dependent CFT component has been already cancelled by the memory cells. Therefore, the fully-differential SI circuit in Fig. 2 eliminates all the error sources, as requested for high performance analog signal processing applications.

3. Performance Estimates

The operation of the proposed circuit has been simulated using SABER, with level 2 MOS transistor model for a 1.2 μm standard CMOS process. All switches have the dimensions 1.2/1.2 μm (W/L) while the diode-connected transistor M_1 100/10 μm . The current mirror ratios α_1 and α_2 are set to 1 and 0.5, respectively. All simulations were performed supposing a 5 V power supply and a bias current $J = 100 \mu\text{A}$. Figure 3 shows the balanced output currents for balanced sinusoidal inputs with 20 μA amplitude and 10 μA CM offset. The sampling frequency is 500 kHz. It can be seen that the circuit outputs are well-balanced due to a substantial reduction of the CM and CFT

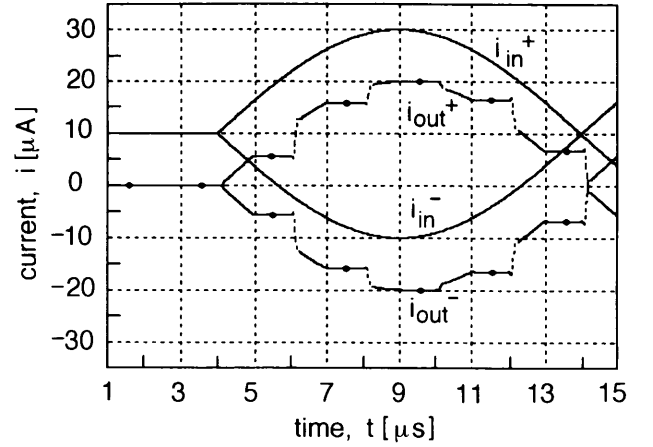


Fig. 3 Simulation results of output currents.

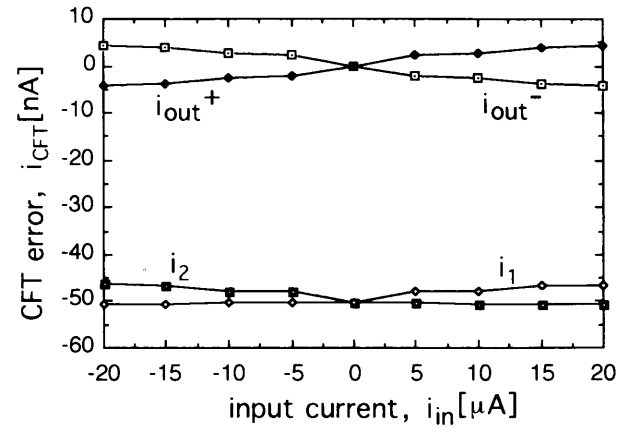


Fig. 4 Simulation results of CFT errors.

components. Figure 4 shows more detailed measurements of the CFT errors. The input is the PWL signal sampled at 100 kHz frequency. The lower traces show the CFT errors in the memory cells. Differing from (6), the errors contain the signal-dependent component. This is because Eq. (1) gives only the first order approximation. The upper traces show that the constant CFT components are completely cancelled and no offset errors appear at the outputs when $i_{in}^+ = i_{in}^- = 0$. The residual CFT errors are less than 0.05% over the range from $-20 \mu\text{A}$ to $20 \mu\text{A}$. This residual error decreases with increasing bias current.

In a practical condition, non-ideal effects such as transistor gain error and threshold mismatch degrade these simulated performances. Their effect on the CMR can be estimated in terms of the mismatch error in current mirrors involved in the memory cells and the current summing circuits. Referring to (7) and noting that the CM input signal i_{CM} is defined by

$$i_{CM} = (i_{in}^+ + i_{in}^-) / 2, \quad (9)$$

one can derive the following expression for the residual CM component δi_{CM} in the output current:

$$\delta i_{CM} = (\varepsilon_M + \varepsilon_S) i_{CM} / 2, \quad (10)$$

where ε_M denotes the mismatch between the current transfer gains of the memory cells and ε_S is that of the

current summing blocks. These errors are independent each other and are evaluated to be 0.4% and 0.2%, respectively, from the current-mirror ratio error [4]. Therefore, the CMR in a practical environment is estimated to be 53 dB.

The non-ideal current mirrors in the memory cells also produce the uncanceled signal-dependent CFT component δi_{CFT} which is given, to first order, by

$$\delta i_{CFT} = \frac{2\varepsilon_{45}(J + i_{in})V_C}{V_{GS1} - V_T} \quad (11)$$

where ε_{45} is the current-mirror ratio error between M_4 and M_5 in Fig. 1. A typical value of ε_{45} is 0.14% [4]. By substituting the parameter values used in the simulations, δi_{CFT} is evaluated to be 7 nA. Because of the two uncorrelated memory cells, the signal-dependent CFT current of 10 nA is superposed on i_{out}^+ and i_{out}^- in Fig. 4. The SNR when $i_{in} = 20 \mu\text{A}$ is therefore estimated to be 63 dB in practice.

4. Conclusions

A new architecture for fully-differential SI circuit was proposed. Because of its high rejection capabilities of

CFT and CM errors, it will be quite useful as a building block for filters, D/A and A/D converters. Adopting the folded cascode structure will further improve its performance.

References

- [1] M. Song, Y. Lee, and W. Kim, "A clock-feedthrough reduction circuit for switched-current systems," *IEEE J. Solid-State Circuits*, vol. 28, no. 2, pp. 133-137, Feb. 1993.
- [2] J. B. Hughes and K. W. Moulding, "S²I: A switched-current technique for high performance," *Electron. Lett.*, vol. 29, no. 16, pp. 1400-1401, Aug. 1993.
- [3] B. Jonsson and S. Eriksson, "New clock-feedthrough compensation scheme for switched-current circuits," *Electron. Lett.*, vol. 29, no. 16, pp. 1446-1448, Aug. 1993.
- [4] C. Toumazou, J. B. Hughes, and N. C. Battersby, "Switched-Currents: an analogue technique for digital technology," chaps. 4 and 6, Peter Peregrinus, London, 1993.
- [5] H. Traff and S. Eriksson, "Novel pseudo-class AB fully differential 3V switched-current system cells," *Electron. Lett.*, vol. 30, no. 7, pp. 536-537, March 1994.
- [6] R. T. Baird, T. S. Fiez, and D. J. Allstot, "Speed and accuracy considerations in switched-current circuits," *Proc. International Symp. Circuits and Systems*, pp. 1809-1812, 1991.